Excited singletstate lifetimes of hydrated chlorophyll aggregates

A. J. Alfano, F. E. Lytle, M. S. Showell, and F. K. Fong

Citation: The Journal of Chemical Physics **82**, 758 (1985); doi: 10.1063/1.448500
View online: http://dx.doi.org/10.1063/1.448500
View Table of Contents: http://scitation.aip.org/content/aip/journal/jcp/82/2?ver=pdfcov
Published by the AIP Publishing

Excited singlet-state lifetimes of hydrated chlorophyll aggregates

A. J. Alfano,[a] F. E. Lytle, M. S. Showell,[b] and F. K. Fong
Department of Chemistry, Purdue University, West Lafayette, Indiana 47907

(Received 28 November 1983; accepted 7 August 1984)

A time-correlated single photon counting technique, coupled with a red sensitive photomultiplier tube, was used to determine the singlet-state lifetimes and energy transfer mechanisms of Chl $a{\cdot}H_2O$, $(\text{Chl } a{\cdot}H_2O)_2$, and $(\text{Chl } a{\cdot}2H_2O)_n$. The use of low concentrations and low incident light fluxes permitted measurements in a regime where nonlinear quenching effects are absent. The lifetimes exhibit a pronounced dependence on aggregate size. The results are examined in terms of exciton interactions in the excited singlet state of the Chl *a* aggregate. It is shown that in the absence of exciton annihilation effects, the rate of singlet-state decay via radiative coupling and intersystem crossing of a Chl *a* aggregate containing *n* equivalent monomeric units is equal to *n* times that of monomeric Chl *a*.

I. INTRODUCTION

The study of *in vitro*[1–6] and *in vivo*[7–9] chlorophyll as well as model compounds[10,11] has been aided by fluorescence quantum yield and lifetime measurements which provide useful information on the excited-state decay kinetics of these systems. An important objective is to establish the photophysical properties that accompany the photoelectrochemical behavior[1,3] of hydrated Chl *a* aggregates and to gain insight into the modeling of photosynthetic reaction centers.[1,11] Picosecond pulsed lasers combined with streak camera detectors were a very welcome tool to investigators delineating the primary processes occurring in the subnanosecond regime.[7] However, the high photon fluxes ($>10^{14}$ photons per pulse) associated initially with the neodymium laser and the photographic streak camera detection process revealed the occurrence of singlet–singlet annihilation in single pulse experiments and also singlet–triplet annihilation in pulse train excitation experiments.[12–16] It is widely recognized[15] that laser pulse intensities less than 10^{13} photons per pulse are in general required to observe fluorescence decay behavior in the absence of nonlinear effects.

The high repetition rate, narrow gated photon counting technique was described[17] as a very reliable means of determining nanosecond to subnanosecond fluorescence lifetimes in dilute and/or low fluorescence quantum yield systems at low photon flux. The synchronously pumped, cavity dumped dye laser employed in this work provides $\sim 10^{10}$ photons per pulse at a wavelength (623 nm) suitable for chlorophyll excitation. In this study the fluorescence temporal decay behavior of three hydrated chlorophyll aggregates Chl $a{\cdot}H_2O$, $(\text{Chl } a{\cdot}H_2O)_2$, and $(\text{Chl } a{\cdot}2H_2O)_n$ was obtained to provide a controlled study of the effect of aggregation state on the chlorophyll fluorescence lifetime *in vitro*. Very high signal-to-noise ratio measurements on these systems required only $\sim 10^8$ photons per pulse at a 5 MHz excitation rate. Previous results show a solvent dependence of the fluorescence lifetime of a covalently linked Chl *a* pair.[10,11] An earlier study in this laboratory[18] involved 337 nm excitation (<35 Hz, $\sim 10^{12}$ photons per pulse) to excite the Soret bands of the monomer Chl $a{\cdot}H_2O$ and polymeric aggregate (Chl $a{\cdot}2H_2O)_n$. In the present work the pulsed laser excitation at 623 nm in conjunction with gated photon counting detection clarifies the earlier results by providing data on the dimeric species $(\text{Chl } a{\cdot}H_2O)_2$. This dimer[19,20] is postulated as a model for the P700 chlorophyll reaction center complex in plant photosynthesis.[1,11] These dimer results also provide a basis for a comparison with the fluorescence decay properties[1] of another P700 model $(\text{Chl } a{\cdot}\text{EtOH})_2$.[21] The observed dependence of fluorescence lifetime on the size of the Chl *a* aggregate is considered in terms of exciton interactions in the excited state.

EXPERIMENTAL

A. Sample preparation

Samples of 10^{-5}–10^{-4} M Chl *a* solution in water-saturated 1:1 methylcyclohexane/*n*-pentane were prepared according to the method described earlier.[1] The samples were deoxygenated in 4 mm o.d. Pyrex glass capillaries by freeze–pump–thaw cycling at 77 K (sample 1: 1×10^{-5} M; sample 2: 2×10^{-5} M; sample 3: 3×10^{-5} M; sample 4: 7×10^{-5} M; sample A: 1×10^{-4} M). The capillaries were hermetically sealed under vacuum ($\sim 10^{-4}$ Torr). Stock chlorophyll *a* purity was established according to the usual criteria.[1] Samples prepared in this way contain principally the monomer and to a lesser extent dihydrate polymer aggregates.[18]

A 4.5×10^{-5} M sample of chlorophyll which yields primarily the monohydrate dimer[1] $(\text{Chl } a{\cdot}H_2O)_2$, upon cooling to 77 K, was prepared according to the procedure of Hoshino *et al.*[22] and sealed under vacuum in a 4 mm o.d. Pyrex capillary (sample B).

B. Time-resolved fluorescence instrumentation

Figure 1 displays the laser source and narrow-gated photon counting detection system for which the background was presented in Ref. 17. The synchronously pumped, cavity dumped rhodamine 6 G dye laser (Coherent 599) was operated at 623 nm and a repetition rate of 5 MHz (50 mW average power). The glass capillaries containing the chlorophyll samples were positioned in an Oxford Instruments DN704 variable temperature (77–300 K) cryostat. Temperatures below ambient were maintained to within ± 1 degree of the desired value with a temperature controller built in this laboratory. Temperature measurements were made with an

[a] Present address: Rockwell Science Center, Thousand Oaks, CA 91360.
[b] Present address: Ivorydale Technical Center, Procter and Gamble Co., Cincinnati, OH 45217.

 0021-9606/85/020758-07$02.10

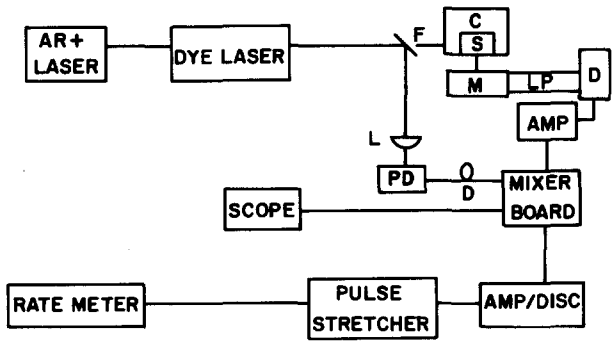

FIG. 1. Laser excitation source and gated photon counting detection system. Dye laser is a synchronously pumped, cavity dumped unit operated at 5 MHz; F, neutral density filters (typical transmission 0.1%); AMP/DISC, ORTEC 9301 preamp and Canberra 1428 A constant fraction discriminator; AMP, 500 MHz bandwidth rf amplifier; C, variable temperature cryostat; S, sample holder; M, 0.25 meter monochromator; LP, lens pair; D, photomultiplier; L, focusing lens; PD, fast photodiode; D, variable delay trombone line; MIXER BOARD, microwave quality substrate containing a double balanced mixer, resistive power divider, and impedance matching circuitry.

Omega platinum RTD mounted directly above a specially machined brass sample holder. Sample fluorescence at 90° from the line of excitation was imaged onto the entrance slit of an 0.25 m Jarrell–Ash monochromator. Wavelength-selected light from the monochromator exit slit was focused to a submillimeter diameter spot on the detector photocathode by a lens pair in an effort to minimize the photomultiplier tube (PMT) transit time spread.[23] Careful adjustment was necessary to ensure illumination of a photocathode region which provided the lowest overall instrument response function. A Corning CS 2-64 filter preceded the monochromator to exclude the scattered laser line. The detector was an uncooled, red-sensitive Hamamatsu R446 photomultiplier which was specially wired and evaluated for photon counting. A recent report[23] documented the capabilities of the R928 (a high anode and cathode sensitivity variant of the R446) in a time-correlated single photon counting application, but no single electron response (SER) or pulse height distribution (PHD) data were cited.

A high speed base and a dynode voltage divider were constructed on 1/32 in, one ounce copper-clad Teflon–glass circuit board (RT Duroid, Rogers Corporation, Chandler, AZ). One side of the board served as a ground plane. The R446 tube base was removed by carefully sawing around the periphery near the bottom of the glass envelope and subsequently desoldering the pins. (Hamamatsu tubes show a remarkable resistance to attempts to eliminate the glass to base seal with solvent.) The metal leads through the glass envelope were then shortened and soldered directly to the circuit board base. The anode pin was soldered to a 50 Ω microstripline trace which was terminated with 50 Ω coax cable. The tube envelope was coated with conductive paint and connected through a 10 MΩ resistor to cathode potential. The applied dynode voltage ($-$ 1500 V) was divided with a cathode to D_1 resistance of 727 K Ω and all other resistors were 220 K Ω. The interelectrode parasitic capacitances ($\sim$6 pF) served as charge storage elements.

The single electron response at a total applied voltage of $-$ 1500 V had a full width at half-maximum (FWHM) of 1100 ps and a peak height of $\sim$270 mV. In order to clearly distinguish a photon-initiated pulse from the electronic noise and thermionic emission along the dynode string, a minimum applied voltage of $-$ 1300 V was required. This potential exceeds the recommended maximum of $-$ 1250 V. The differential and integral PHD at $-$ 1300 V provide a peak to valley ratio of 3.8 and a FWHM to most probable peak height ratio of 1.8. The PMT was operated at $-$ 1500 V with a large cathode to first dynode voltage (403 V) in order to minimize the wavelength dependence of its temporal characteristics.[23,24]

Detector output pulses were amplified by a factor of 22 with a TRW CA2820 wideband rf amplifier and then attenuated by a factor of 10 with a General Radio 874-G20 attenuator. This provided $\sim$600 mV pulses of 1200 ps FWHM at the rf port of the double balanced mixer. The severe ringing associated with narrow-pulsed operation of the rf amplifier was reduced to 11% of peak by terminating the PMT pulses at the amplifier input pin with a 120 Ω resistor to ground and a series inductor to the amplifier consisting of two turns (0.6 cm diam) of 18 gauge copper wire. The amplifier was mounted to microstripline traces on RT Duroid circuit board. Power supply decoupling components were as specified by the TRW data sheet.

C. Fluorescence spectra

Fluorescence spectra, uncorrected for the PMT spectral response, were obtained with the laser source (623 nm) and the collection geometry shown in Fig. 1. The detector output was fed directly to a Keithley 427 current amplifier and recorded on a 7100B Hewlett–Packard strip chart. Wavelength was scanned with a stepping motor unit attached to the 0.25 m monochromator.

III. RESULTS

A. Fluorescence spectra

The fluorescence spectra of five different samples are shown in Fig. 2. Spectra at room temperature and at a temperature between 85 and 100 K were recorded for each sample. Fluorescence bands at 671–674 nm at room temperature and at 684 nm at low temperatures, attributable to Chl $a{\cdot}H_2O$, are observed.[18] The room temperature fluorescence of $(\text{Chl } a{\cdot}2H_2O)_n$, visible at 764 nm,[18,25] is detected only in the two most concentrated samples. At low temperature a shoulder at 749 nm is seen in the most dilute preparation at wavelengths to the red of 684 nm. At increased concentration this shoulder appears to red shift gradually to form the unsymmetrical band at $\sim$760 nm. A shoulder at 728 nm in the ambient low-concentration spectrum (sample 1) shifts to the low-temperature shoulder at 749 nm.

In Fig. 3 the ambient and low-temperature fluorescence spectrum of sample B is reproduced. This sample exhibits a shift in the fluorescence maximum, from 672 to 725 nm upon cooling, indicative of $(\text{Chl } a{\cdot}H_2O)_2$ formation from Chl $a{\cdot}H_2O$.[19,22] The fluorescence spectra of the most concentrated polymer sample (A) from Fig. 2 is shown in Fig. 3 for comparison. It is noted that the blue side of the monomer

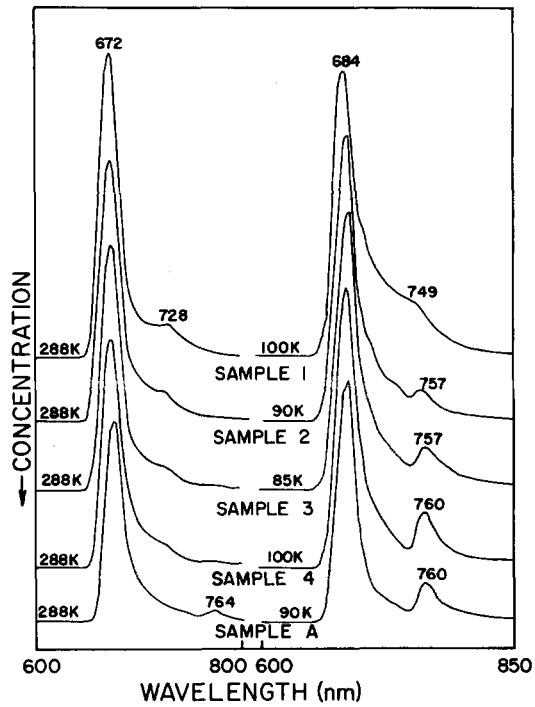

FIG. 2. Concentration dependence of chlorophyll fluorescence spectra at ambient and low temperatures.

fluorescence band in all spectra is affected by the presence of the CS 2-64 filter for eliminating the scattered laser line.

B. Time-resolved fluorescence decay

The response function of the photon counting apparatus (Fig. 1) was obtained with the 623 nm excitation wavelength by scattering from the chlorophyll samples which contain the polymeric aggregate. These preparations are most accurately considered as suspensions of polycrystalline (Chl a·$2H_2O)_n$ in the water-saturated nonpolar solvent.[1,18] Figure 4 shows a typical instrument response along with the 288 K fluorescence decay profile of Chl a·H_2O at 676 nm from sample A. The temperature dependence of the monomer fluorescence lifetime appears in the inset. The narrow instrument response obviates the need for deconvolution in this case and permits simple weighted regression for lifetime recovery.

Figure 5 demonstrates the lifetime behavior of sample B at 288, 130, and 77 K with the fluorescence detected at 733, 736, and 738 nm, respectively.

Figure 6 reproduces the results obtained for polymer fluorescence at 774 nm from samples 1 (100 K), 2 (80 K), and A (94 K). It is clear that a longer-lived fluorescent decay component dominates at lower Chl a concentration and that rapid decay kinetics prevail at higher Chl a concentrations.

The time-resolved fluorescence decay of sample A at 774 nm is shown for two temperature extremes 288 and 77 K in Fig. 7. The instrument response at 623 nm is also indicated. This sample accentuates the rapid (Chl a·$2H_2O)_n$ fluorescence decay kinetics. Detectable fluorescent signal extends out to ~14 ns in samples 1–4 and A with detection in the 765–774 nm region of the polymer band.

IV. DISCUSSION

The results in Fig. 2 are indicative of the increasing extent of temperature-dependent formation of polymeric (Chl a·$2H_2O)_n$, with maximum fluorescence at ~760 nm, from smaller hydrated Chl a complexes[18] with increasing Chl a concentration. All fluorescence decay data for Chl a·H_2O and (Chl a·$H_2O)_2$ were weighted according to Poisson statistics and then least-squares fit to single- or double-exponential decay models. The weighted decay data for (Chl a·$2H_2O)_n$ were compared to computer convolutes of the instrument response function with various decay models using

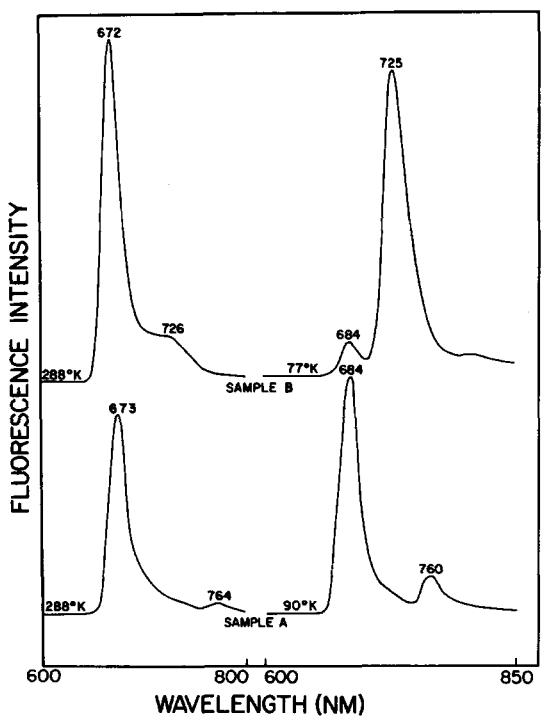

FIG. 3. Fluorescence spectra of chlorophyll monohydrate dimer forming sample (sample B). Corresponding spectra of the most concentrated polymer forming sample (sample A) from Fig. 2 serve as reference.

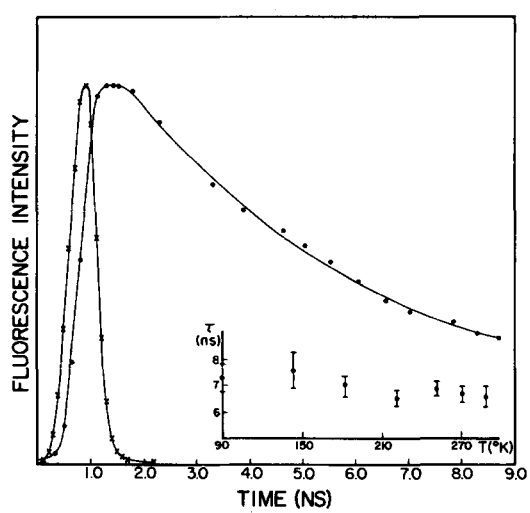

FIG. 4. Instrument response (×) and room temperature fluorescence decay profile (●) for chlorophyll monomer in sample A. Temperature dependence of fluorescence lifetime is shown in the inset.

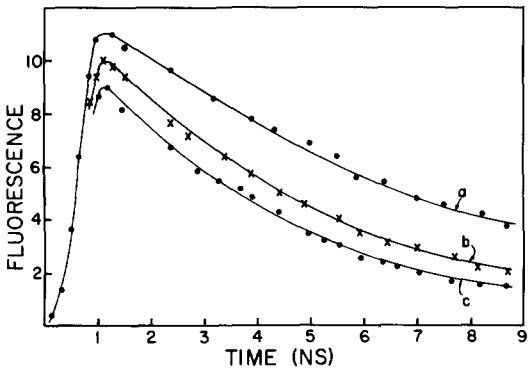

FIG. 5. Temperature dependence of chlorophyll monohydrate dimer fluorescence decay. (a) 288 K, (b) 130 K, and (c) 77 K.

an iterative least squares method.[26] A wavelength disparity of ~150 nm exists between the instrument function (623 nm) used in the deconvolution and (Chl a·$2H_2O$)$_n$ fluorescence decay data (~774 nm). The FWHM of the instrument response function is generally increased at shorter wavelength[24] due to a wavelength-dependent transit time spread of photoelectrons within the PMT. The rising portion of the response function is most affected. A recent study of the wavelength dependence of the temporal response[23] of a detector similar to the R446 showed a 19 ps/100 nm shift in the peak of the instrument function but essentially no change in width. The entire, uncorrected instrument response curve was used here in the iterative convolution with small ($< 1\%$), random residuals resulting. The deconvoluted (Chl a·$2H_2O$)$_n$ lifetimes therefore represent upper limits since wavelength correction of the impulse response would provide shorter, if not identical, lifetimes. In all cases the uncertainties reported are 95% confidence limits on the precision of the fit. The computer program was capable of correctly resolving a 1% contribution of a 200 ps exponential decay in the presence of 99% of a 50 ps exponential for synthetic data.

The time-resolved results for the Chl a·H_2O monomer (Fig. 4) indicate a slight temperature dependence of the fluorescence lifetime averaging to 6.9 ns (6% standard deviation). The monomer lifetimes obtained earlier[18] with 337 nm excitation also exhibit decreasing values with increasing temperatures averaging to 6.9 ns. Fluorescence quenching effects *in vitro* have been reported to have a quadratic dependence on bulk chlorophyll concentration.[6] However, no clear evidence of enhanced quenching (reduced fluorescence lifetime) is found over a tenfold increase in the Chl a concentration at room temperature in Table I. Other investigators report similar monomer lifetimes of 6.2 ns (670 nm),[5] 6.5 ns (688 nm),[5] 6.4 ns (pyridine),[27] 6.05 ns (toluene),[27] and 7.3 ns (pyridine).[2]

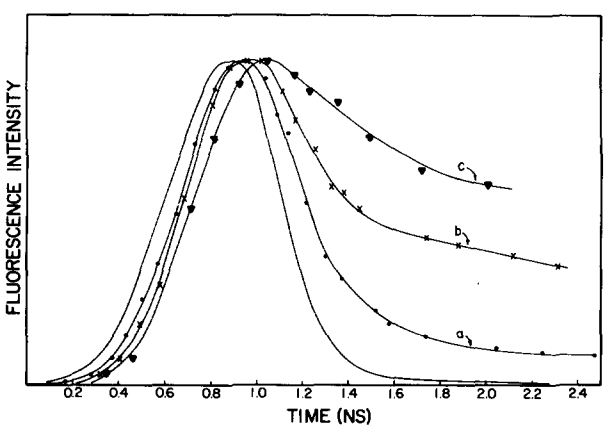

FIG. 6. Instrument response function and concentration dependence of chlorophyll dihydrate polymer fluorescence decay. (a) Sample A, 94 (K); (b) sample 2, 80 (K); (c) sample 1, 100 (K).

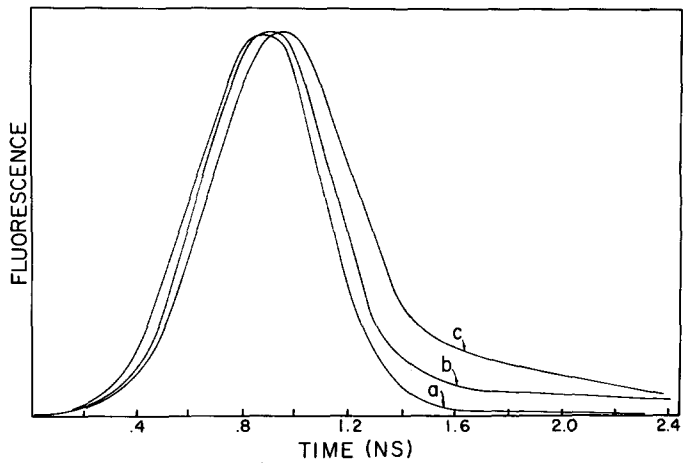

FIG. 7. Instrument response function (a) and dihydrate polymer fluorescence decay from Sample A at (b) 288 K and (c) 77 K.

Sample B contains principally Chl a·H_2O in 3-methylpentane at room temperature and yields (Chl a·H_2O)$_2$ upon cooling as the equilibrium 2Chl a·H_2O⇌(Chl a·H_2O)$_2$ shifts to the right.[19,22] This is accompanied by a shift in the 672 nm fluorescence maximum (Fig. 3) for monomeric Chl a·H_2O[18] to a maximum at 725 nm, which is characteristic of (Chl a·H_2O)$_2$.[19,22] The apparent temperature dependence of the fluorescence lifetime observed in Fig. 5 is thus attributed to a change in sample composition as dimers are formed from monomers rather than an increase in the monomer fluorescence decay rate at lower temperatures. The fluorescence lifetime monitored at 666 nm at 288 K and 676 nm at 77 K is 6.8 ± 0.2 and 6.3 ± 0.2 ns, respectively. Figure 3 displays a drastic change in dimer concentration between 288 and 77 K while the monomer fluorescence lifetime changes by only 0.5 ns.

The fluorescence lifetime obtained from the data in Fig. 5 (730–740 nm region) are 6.7 ± 0.2 (288 K), 4.6 ± 0.1 (130 K), and 3.9 ± 0.3 ns (77 K). It is quite likely that fluorescence from Chl a·H_2O extends into this region and an average lifetime was obtained which is heavily weighted predominantly toward the monomer at room temperature and the dimer at 77 K, in accordance with the fluorescence spectra in Fig. 3. A double exponential decay model of the form

$$I_F = A \exp(-t/3.7 \text{ ns}) + (1-A)\exp(-t/6.9 \text{ ns}) \quad (1)$$

for the fluorescence intensity I_F was found to yield random residuals at all three temperatures with $A = (8 \pm 8)\%$, $(75 \pm 4)\%$, and $(95 \pm 4)\%$ at 288, 130, and 77 K, respectively. The value of 6.9 ns corresponds to the fluorescence lifetime of Chl a·H_2O, while the corresponding value for (Chl a·H_2O)$_2$ is 3.7 ns. Temperature dependencies of the deconvoluted absorption spectra, fluorescence specta, and fluorescence lifetimes were reported on chlorophyll systems in non-

TABLE I. Chl *a* monomer fluorescence lifetime at various concentrations.

Sample	Chl *a* (M)[a]	T(K)	λ (nm)	τ(ns)
1	1×10^{-5}	287	666	7.3 ± 0.6
2	2×10^{-5}	287	666	6.9 ± 0.3
3	3×10^{-5}	285	666	6.0 ± 0.4
4	7×10^{-5}	287	666	6.9 ± 0.3
A	1×10^{-4}	288	676	6.5 ± 0.4

[a] Total Chl *a* concentration in the sample based on spectrophotometric analysis of Chl *a* in anhydrous ethyl ether.

polar solvents with ethanol rather than water as a nucleophile.[6] The monomer fluorescence lifetime was found to be independent of temperature at 670 nm, while below 233 K the lifetime at 725 nm (4.1 ns average) was dominated by a single contributor to the deconvoluted absorption spectrum beyond 700 nm. The similarity of the 3.7 and 4.1 ns lifetimes supports the assignment of the latter lifetime to (Chl *a*·ETOH)$_2$.[21]

The long-lived component in Figs. 6 and 7 has an average value of 6.7 ns and thus corresponds to the monomer fluorescence lifetime. In view of the fact that Fig. 2 suggests a negligible contribution of the monomer fluorescence beyond 760 nm, the presence of the 6.7 ns component suggests excitation transfer from the monomer to the polymer. A reasonable decay law for use in the deconvolution of the polymer fluorescence in the 0–2.4 ns region is of the form

$$I_F = A\exp(-t/\tau) + B\exp(-t/6.9\ \text{ns}) + C\exp(-t/3.7\ \text{ns}), \tag{2}$$

where the first term corresponds to the lifetime component attributable solely to (Chl *a*·2H$_2$O)$_n$. The second and third terms in Eq. (2) denote contributions to the fluorescence decay from Chl *a*·H$_2$O and (Chl *a*·H$_2$O)$_2$, respectively. The deconvoluted fluorescence lifetime τ for the data shown in Fig. 7 and for data at several intermediate temperatures is given in Table II. Although an undefined temperature-dependent distribution of aggregational states is represented by (Chl *a*·2H$_2$O)$_n$,[18] Table II indicates that a single fluorescence lifetime persists between 288 and 179 K. Below 179 K the lifetime increases to 112 ps and a more complicated decay model is clearly required. The earlier polymer study[18] showed a similar temperature dependence which agrees with the current room temperature result, but indicates a 600 ps lifetime below 125 K. The (Chl *a*·2H$_2$O)$_n$ absorption and fluorescence band is a complex, temperature-dependent composite arising from a distribution of aggregate sizes given by n. In the discussion to follow, it is shown that the aggregate size has a pronounced effect on the excited-state lifetime of the chlorophyll.

TABLE II. Temperature dependence of (Chl *a*·2H$_2$O)$_n$ fluorescence lifetime at 774 nm.

T(K)	τ(ps)	A
288	54 ± 7	99%
260	54 ± 9	99%
230	68 ± 7	99%
200	63 ± 5	98%
179	69 ± 4	98%
140	94 ± 7	97%
95	103 ± 11	97%
77	112 ± 12	97%

Molecular systems of the type (Chl *a*·2H$_2$O)$_n$ possess structures having one-dimensional periodicity. The individual Chl *a* units are generated by repetition of the hydrated monomeric units in translational symmetry.[1] A model of the excited states of (Chl *a*·2H$_2$O)$_n$ developed in a manner analogous to that used to treat excitons in crystalline solids[28] can be employed to account for the observed dependence of fluorescence lifetime on the Chl *a* aggregate size (Figs. 4–7).

The singlet-state wave function for a linear exciton system of infinite length may be written[29]

$$|\psi_{S_1\kappa_\nu}\rangle = \sum_j \exp(i\kappa_\nu\cdot\mathbf{R}_j)|\chi_{S_1}(j)\rangle, \tag{3}$$

where

$$|\chi_{S_1}(j)\rangle = |\Phi_{S_1}(j)\rangle\prod_{i\neq j}|\Phi_{S_0}(i)\rangle \tag{4}$$

gives the jth monomeric unit in the excited singlet state $|\Phi_{S_1}(j)\rangle$. In Eq. (3) κ_ν is a wave vector and $\mathbf{R}_j = j\hat{a}$, a position vector, is given by integral multiples of the unit vector $\hat{a}$. The linear combination of $|\psi_{S_1\kappa_\nu}\rangle$ with its complex conjugate gives

$$|\psi'_{S_1\kappa_\nu}\rangle = \sum_{j=1}^{n}\sin(\kappa_\nu\cdot\mathbf{R}_j)|\chi_{S_1}(j)\rangle \tag{5}$$

which satisfies the boundary conditions $\langle\chi_{S_1}(0)|\psi'_{S_1\kappa_\nu}\rangle = \langle\chi_{S_1}(n+1)|\psi'_{S_1\kappa_\nu}\rangle = 0$ given $\kappa_\nu = \pi\nu\hat{a}/(n+1)$, with $\nu = 1,2,\ldots,n$.

There are two principal contributions to the decay of the S_1 state, viz., radiative decay to S_0 and intersystem crossing to T_1. We assume zeroth-order product states for S_0[28–30]:

$$|\psi_{S_0}\rangle = \prod_j|\Phi_{S_0}(j)\rangle \tag{6}$$

and for T_1:

$$|\psi_{T_1}\rangle = |\Phi_{T_1}(j)\rangle\prod_{i\neq j}|\Phi_{S_0}(i)\rangle. \tag{7}$$

In writing Eq. (7) we have assumed that exciton interactions in the T_1 state of (Chl *a*·2H$_2$O)$_n$ are negligibly small.[31] We define the transition matrix elements

$$\langle\psi'_{S_1\kappa_\nu}|\hat{\mu}|\psi_{S_0}\rangle = \mu(Q_j) \tag{8}$$

for radiative decay through the electric dipole coupling operator $\hat{\mu}$ and

$$\langle\psi'_{S_1\kappa_\nu}|\mathbf{s}\cdot\mathbf{l}|\psi_{T_1}\rangle = \Omega(Q_j) \tag{9}$$

for intersystem crossing via spin-orbit interaction $\mathbf{s}\cdot\mathbf{l}$. In Eqs. (8) and (9) Q_j denotes collectively the vibrational coordinates of the jth Chl a unit.

The $\mu(Q_j)$ and $\Omega(Q_j)$ in Eqs. (8) and (9) can be expanded in Taylor series[30] about the S_1 equilibrium positions Q^0_{ij} for the ith modes of the jth monomeric unit. Assuming the leading terms in the expansions $\mu(Q^0_j)$ and $\Omega(Q^0_j)$ give the dominant contributions to S_1 decay, we obtain

$$\langle \psi'_{S_1\kappa_\nu}|\hat{\mu}|\psi_{S_0}\rangle = A\sum_{j=1}^{n}\sin[j\pi\nu/(n+1)]\mu(Q^0_j) \tag{10}$$

and

$$\langle \psi'_{S_1\kappa_\nu}|\mathbf{s}\cdot\mathbf{l}|\psi_{T_1}\rangle = A\sum_{j=1}^{n}\sin[j\pi\nu/(n+1)]\Omega(Q^0_j), \tag{11}$$

where

$$A = \left\{\sum_{j=1}^{n}\sin^2[j\pi\nu/(n+1)]\right\}^{-1/2}$$

is a normalization constant obtained from the condition $\langle \psi'_{S_1\kappa_\nu}|\psi'_{S_1\kappa_{\nu'}}\rangle = \delta_{\nu\nu'}$.

Equations (10) and (11) can be used to predict the decay rates W_n of hydrated Chl a aggregates relative to that W_1 of Chl $a\cdot H_2O$. For a dimer, such as (Chl $a\cdot H_2O)_2$ composed of two equivalent monomeric units, i.e., $n=2$ and $\mu(Q^0_1) = \mu(Q^0_2)$, Eqs. (10) and (11) simplify to

$$W_2(\mu) \propto |\langle \psi'_{S_1\kappa_\nu}|\hat{\mu}|\psi_{S_0}\rangle|^2 = 2\mu^2 \propto 2W_1(\mu) \tag{12}$$

and

$$W_2(\Omega) \propto |\langle \psi'_{S_1\kappa_\nu}|\hat{\Omega}|\psi_{T_1}\rangle|^2 = 2\Omega^2 \propto 2W_1(\Omega), \tag{13}$$

where $W(\mu)$ and $W(\Omega)$, respectively, denote the radiative and intersystem crossing decay rates. It follows that

$$W_2 = W_2(\mu) + W_2(\Omega) = 2[W_1(\mu) + W_1(\Omega)] = 2W_1. \tag{14}$$

Thus the dimer S_1 decay rates via electric dipole and spin-orbit couplings are twice the corresponding rates of the monomer, in reasonable agreement with the 3.7 and 6.9 ns lifetimes observed for (Chl $a\cdot H_2O)_2$ and Chl $a\cdot H_2O$, respectively. The oligomerization of the chlorophyll into a chain aggregate (Chl $a\cdot 2H_2O)_n$, results in the spreading of single monomeric states into an energy band. The translational symmetry of the aggregate is described by the wave vector κ_ν.[29] The levels in allowed transitions involving the ground state are given by $\kappa_\nu \simeq 0$.[32] In that case it can be shown from Eqs. (10) and (11) that for an aggregate composed of n monomeric units we have

$$W_n = W_n(\mu) + W_n(\Omega) = \Sigma_\nu W_\nu = nW_1, \tag{15}$$

where the sum is taken over the individual rates W_ν arising from the exciton states. The predicted increase in the decay rate of the Chl a S_1 state with increasing aggregate size thus accounts for the experimental results given in Tables I and II and Figs. 4–7. At 288 K, the fluorescence lifetime of (Chl $a\cdot 2H_2O)_n$ is 54 ps (Table II) compared to 6.5 ns for the monomer (Table I), yielding an average aggregate size of $n \sim 120$. This estimate does not take into account any lifetime shortening by quenching effects arising from singlet–triplet annihilation.[25]

In writing Eqs. (12) and (13) the phase factors associated with the dimer wave functions are arbitrarily chosen so the transition matrix elements in Eqs. (8) and (9) are real. Equations (12) and (13) reflect the dependence of the relaxation rates on the orientation of the transition moments.[32] Furthermore, Eqs. (12) and (13) are based on the assumption that the Franck–Condon factor for transitions in aggregated chlorophyll hydrate is approximately the same as that for the monomeric chlorophyll. This assumption implies that the vibrational modes resulting from Chl a aggregation do not contribute to electronic transitions as accepting modes. The intermolecular interactions that give rise to Chl a aggregation involve hydrogen bonding between the ring V carbonyl groups and the centrally ligated water molecules of neighboring monomeric units.[1,4,33] The resulting normal modes absorb in the 3000–3800 cm^{-1} wavelength region.[33] The validity of the above treatment is evidently corroborated by the observed doubling of the (Chl $a\cdot H_2O)_2$ S_1 decay rate compared to that of monomeric Chl $a\cdot H_2O$.

The above considerations provide sharp contrast to the observed relaxation behavior of certain excimeric aromatic hydrocarbons in which the molecular aggregates are held together by weak van der Waals interactions.[34,35] For example, the room-temperature fluorescence lifetime of excimeric napthalene in cyclohexane is 117 ns, indistinguishable from that, 120 ns, for the corresponding monomer.[34] On the other hand, a reduction in the phosphorescence lifetime, from 79 ± 5 to 41 ± 5 ms, has been observed upon dimerization of 1,4-dibromonaphthalene.[36]

In living systems a large portion of Chl molecules function as antenna which absorb photons and then transfer the resultant singlet energy to specialized Chl a molecules in the photosynthetic reaction center. The Förster mechanism has been widely invoked to explain this energy transfer.[37–39] This mechanism has a critical distance dependence and therefore is favored at high concentration. The chlorophyll concentration in green plant membranes is $> 10^{-3}$ M,[40] more than one order of magnitude greater than that employed in the present study. The results in Table I do not indicate that this mechanism is operative here. The presence of the invariant monomer and dimer lifetimes in Eq. (2) in the deconvolution of (Chl $a\cdot 2H_2O)_n$ fluorescence decay suggests the possibility of radiative energy transfer between the bluer absorbing and the lower-energy absorbing aggregates.

From Table II it is evident that the contribution of this mechanism is less than 3% of the total fluorescence observed. The water molecule in Chl $a\cdot H_2O$ denotes that bonded to the Chl a Mg atom on the same side of the macrocycle as the C-10 carbomethoxy group responsible for aggregation interactions.[1] A second water of complexation to Mg in monomeric Chl a can occur on the opposite side of the macrocycle as manifested by the observation[18] of oscillatory delayed fluorescence attributable only to monomeric Chl a in water-saturated nonpolar solutions.[41] In the samples employed in this study the observed fluorescence originates predominantly from monomeric Chl a. Significantly, in a sample containing primarily polycrystalline Chl a (Chl $a\cdot 2H_2O)_n$, extensive fluorescence quenching due to singlet–triplet annihilation effects is observed.[25] In addition to singlet–triplet annihilation effects, the dramatic decrease in the

fluorescence quantum efficiency of polycrystalline Chl *a*, $(\text{Chl } a \cdot 2H_2O)_n$, noted in an earlier study,[18] is evidently explainable, in view of Eq. (15), in terms of the enhanced rate of intersystem crossing due to S_1 exciton interactions obtained upon aggregation of the chlorophyll. The dependence of the photophysical properties of excited Chl *a* on the state of aggregation provides contrast and comparison with that of photochemical effects described previously.[1,41]

ACKNOWLEDGMENTS

This work was supported by the Basic Research Division of the Gas Research Institute (FKF) and the National Science Foundation (FEL).

[1]F. K. Fong, in *Light Reaction Path of Photosynthesis*, edited by F. K. Fong (Springer, New York, 1982), Chap. 8.
[2]J. C. Hindman, R. Kugel, M. R. Wasielewski, and J. J. Katz, Proc. Natl. Acad. Sci. U. S. A. **75**, 2076 (1978).
[3]O. Inganas and I. Lundstrom, J. Appl. Phys. **54**, 4185 (1983); F. K. Fong and L. Galloway, J. Am. Chem. Soc. **100**, 3594 (1978); D. R. Fruge, G. D. Fong, and F. K. Fong, *ibid.* **101**, 3694 (1979).
[4]R. J. Abraham and K. M. Smith, J. Am. Chem. Soc. **105**, 5734 (1983).
[5]G. R. Seely and V. Senthllathlpan, J. Phys. Chem. **87**, 373 (1983).
[6]M. J. Yuen, L. L. Shipman, J. J. Katz, and J. C. Hindman, Photochem. Photobiol. **36**, 211 (1982); M. J. Yuen, L. L. Shipman, J. J. Katz, and J. C. Hindman, *ibid.* **32**, 281 (1980).
[7]J. Breton and N. E. Geacintov, Biochim. Biophys. Acta **594**, 1 (1980).
[8]W. Haehnel, J. Nairn, P. Reisberg, and K. Sauer, Biochim. Biophys. Acta **680**, 161 (1982).
[9]K. Kamogawa, J. M. Morris, Y. Takagi, N. Nakashima, K. Yoshihara, and I. Ikegami, Photochem. Photobiol. **37**, 207 (1983).
[10]M. J. Pellin, M. R. Wasielewski, and K. J. Kaufmann, J. Am. Chem. Soc. **102**, 1868 (1980).
[11]M. R. Wasielewski, in Ref. 1, Chap. 7.
[12]G. Porter, J. A. Synowiec, and C. J. Tredwell, Biochim. Biohys. Acta **459**, 329 (1977).
[13]C. J. Tredwell, J. A. Synowiec, G. F. W. Searle, G. Porter, and J. Barber, Photochem. Photobiol. **28**, 1013 (1978).
[14]N. E. Geacintov, J. Breton, C. Swenberg, A. J. Campillo, R. C. Hyer, and S. L. Shapiro, Biochim. Biophys. Acta **461**, 306 (1977).
[15]A. J. Campillo and S. L. Shapiro, Photochem. Photobiol. **28**, 975 (1978).
[16]F. Pellegrino, W. Yu, and R. R. Alfano, Photochem. Photobiol. **28**, 1007 (1978).
[17]A. J. Alfano, F. K. Fong, and F. E. Lytle, Rev. Sci. Instrum. **54**, 967 (1983).
[18]F. K. Fong, M. Kusunoki, L. Galloway, T. G. Matthews, F. E. Lytle, A. J. Hoff, and F. A. Brinkman, J. Am. Chem. Soc. **104**, 2759 (1982).
[19]F. K. Fong and V. J. Koester, Biochim. Biophys. Acta, **423**, 52 (1976).
[20]F. K. Fong, Proc. Natl. Acad. Sci. U. S. A. **71**, 3692 (1974).
[21]L. L. Shipman, T. M. Cotton, J. R. Norris, and J. J. Katz, Proc. Natl. Acad. Sci. U. S. A. **73**, 1791 (1976).
[22]M. Hoshino, K. Ikehara, M. Imamura, H. Seki, and Y. Hama, Photochem. Photobiol. **34**, 75 (1981).
[23]S. Kinoshita and T. Kushida, Rev. Sci. Instrum. **53**, 469 (1982).
[24]P. Wahl, J. C. Auchet, and B. Donzel, Rev. Sci. Instrum. **45**, 28 (1974).
[25]A. J. Alfano and F. K. Fong, J. Am. Chem. Soc. **104**, 2767 (1982).
[26]A. Grinvald and I. Z. Steinberg, Anal. Biochem. **59**, 583 (1974).
[27]J. S. Connolly, A. F. Janzen, and E. B. Samuel, Photochem. Photobiol. **36**, 559 (1982).
[28]J. N. Turlet, Ph. Kottis, and M. R. Philpott, Adv. Chem. Phys. **LIV**, 305 (1983).
[29]F. K. Fong and W. A. Wassam, J. Am. Chem. Soc. **99**, 2375 (1977).
[30]K. F. Freed, J. Am. Chem. Soc. **102**, 3130 (1980).
[31]A. J. Alfano, M. S. Showell, and F. K. Fong, J. Chem. Phys. **81**, 765 (1984).
[32]D. P. Craig and S. H. Walmsley, *Excitons in Molecular Crystals* (Benjamin, New York, 1968).
[33]K. Ballschmiter and J. J. Katz, J. Am. Chem. Soc. **91**, 2661 (1969).
[34]N. Mataga, M. Tomura, and H. Nishimura, Mol. Phys. **9**, 367 (1965).
[35]H.-H. Perkampus and H. Stichtenoth, Z. Phys. Chem. **76**, 18 (1971).
[36]A. H. Zewail, D. D. Smith, and J. P. Lemaistre, in *Excitons*, edited by E. I. Rashba and M. D. Sturge (North-Holland, Amsterdam, 1982), Vol. 2, Chap. 15.
[37]T. S. Rahman and R. S. Knox, Phys. Status Solidi **58**, 715 (1973).
[38]L. L. Shipman and D. L. Housman, Photochem. Photobiol. **29**, 1163 (1979).
[39]T. G. Monger and W. W. Parson, Biochim. Biophys. Acta **460**, 393 (1977).
[40]P. S. Nobel, in *Introduction to Biophysical Plant Physiology* (Freeman, San Francisco, 1974), p. 201.
[41]M. Kusunoki and F. K. Fong, Chem. Phys. Lett. **102**, 244 (1983).